Carbonylation of Adipose Proteins in Obesity and Insulin Resistance

IDENTIFICATION OF ADIPOCYTE FATTY ACID-BINDING PROTEIN AS A CELLULAR TARGET OF 4-HYDROXYNONENAL*[S]

Paul A. Grimsrud‡, Matthew J. Picklo, Sr.§, Timothy J. Griffin‡, and David A. Bernlohr‡¶

Obesity is a state of mild inflammation correlated with increased oxidative stress. In general, pro-oxidative conditions lead to production of reactive aldehydes such as *trans*-4-hydroxy-2-nonenal (4-HNE) and *trans*-4-oxo-2-nonenal implicated in the development of a variety of metabolic diseases. To investigate protein modification by 4-HNE as a consequence of obesity and its potential relationship to the development of insulin resistance, proteomics technologies were utilized to identify aldehyde-modified proteins in adipose tissue. Adipose proteins from lean insulin-sensitive and obese insulin-resistant C57Bl/6J mice were incubated with biotin hydrazide and detected using horseradish peroxidase-conjugated streptavidin. High carbohydrate, high fat feeding of mice resulted in a ~2–3-fold increase in total adipose protein carbonylation. Consistent with an increase in oxidative stress in obesity, the abundance of glutathione *S*-transferase A4 (GSTA4), a key enzyme responsible for metabolizing 4-HNE, was decreased ~3–4-fold in adipose tissue of obese mice. To identify specific carbonylated proteins, biotin hydrazide-modified adipose proteins from obese mice were captured using avidin-Sepharose affinity chromatography, proteolytically digested, and subjected to LC-ESI MS/MS. Interestingly enzymes involved in cellular stress response, lipotoxicity, and insulin signaling such as glutathione *S*-transferase M1, peroxiredoxin 1, glutathione peroxidase 1, eukaryotic elongation factor 1α-1 (eEF1α1), and filamin A were identified. The adipocyte fatty acid-binding protein, a protein implicated in the regulation of insulin resistance, was found to be carbonylated *in vivo* with 4-HNE. *In vitro* modification of adipocyte fatty acid-binding protein with 4-HNE was mapped to Cys-117, occurred equivalently using either the *R* or *S* enantiomer of 4-HNE, and reduced the affinity of the protein for fatty acids ~10-fold. These results indicate that obesity is accompanied by an increase in the carbonylation of a number of adipose-regulatory proteins that may serve as a mechanistic link between increased oxidative stress and the development of insulin resistance. ***Molecular & Cellular Proteomics 6:624–637, 2007.***

Reactive oxygen species (ROS)[1] and reactive nitrogen species are generated as a result of normal metabolic processes in the cell, including the uncoupling of the electron transport chain in the mitochondria and the oxidation of excess NADPH by NADPH oxidase (1). Oxidative stress occurs due to increased pro-oxidative conditions or the decline of antioxidant systems and is highly correlated with a wide variety of inflammatory and metabolic disease states, including Alzheimer disease, macular degeneration, lung dysfunction, and obesity-linked insulin resistance (2–5). Although the precise role of oxidative stress in disease mechanisms is not completely understood, ROS are known to be highly reactive with proteins, DNA, carbohydrates, and lipids in the cell. The ROS-initiated peroxidation of polyunsaturated acyl chains of membrane phospholipids can result in a Hock cleavage and the subsequent formation of lipid-derived reactive aldehydes (6).

Of the variety of reactive aldehydes formed from lipid peroxidation, *trans*-4-hydroxy-2-nonenal (4-HNE) and *trans*-4-oxo-2-nonenal (4-ONE) have significant contributions to oxidative disease due to their high abundance and strong reactivity (6–9). 4-HNE specifically is metabolized (detoxified) by being reduced to an alcohol (aldehyde reductase), oxidized to a carboxylic acid (aldehyde dehydrogenase), or conjugated to glutathione (glutathione *S*-transferase) (10–12). However, some fraction of 4-HNE escapes metabolism and forms adducts with other nucleophiles including both protein and DNA. In the case of protein, 4-HNE reacts avidly with the side chains of cysteine and histidine residues as well as lysine

From the ‡Department of Biochemistry, Molecular Biology and Biophysics, The University of Minnesota, Minneapolis, Minnesota 55455 and §Department of Pharmacology, Physiology, and Therapeutics, University of North Dakota School of Medicine and Health Science, Grand Forks, North Dakota 58203

Received, April 5, 2006, and in revised form, December 19, 2006

Published, MCP Papers in Press, January 6, 2007, DOI 10.1074/mcp.M600120-MCP200

[1] The abbreviations used are: ROS, reactive oxygen species; A-FABP, adipocyte fatty acid-binding protein (also referred to as aP2); E-FABP, epithelial fatty acid-binding protein (also referred to as KLBP or Mal-1); 4-HNE, *trans*-4-hydroxy-2-nonenal (also referred to as 4-hydroxynonenal); 4-ONE, *trans*-4-oxo-2-nonenal; 1,8-ANS, 1-anilinonaphthalene 8-sulfonic acid; PBST, PBS containing 0.05% Tween 20; ER, endoplasmic reticulum; HRP, horseradish peroxidase; GSTA4, glutathione *S*-transferase A4 (also referred to as GSTA4-4 or GSTa4); βME, β-mercaptoethanol; JNK, c-Jun N-terminal kinase; eEF1α1, eukaryotic elongation factor 1α-1.

albeit to a far lesser extent (13). Although the reactive lipid is formed in membranes, it can diffuse into the cytoplasm and nucleus due to its relatively high solubility, allowing it to react with proteins localized far away from the initial site of oxidative formation (14).

4-HNE modification of protein has been shown to have a variety of effects on its targets. Alkylation by 4-HNE frequently inhibits the activity of enzymes; examples include the Na^+-K^+-ATPase and $NADP^+$-dependent isocitrate dehydrogenase (15, 16). In some cases, however, 4-HNE modification has been suggested to increase the activity of key regulatory proteins such as the dimerization and ligand-independent activation of the epidermal growth factor receptor (17) or the activation of the Nrf2 (nuclear factor erythroid 2-related factor 2) transcription factor, leading to increased expression of genes implicated in the antioxidant response (18–20). In addition to altering the activity of enzymes, 4-HNE alkylation has been shown to alter the rate of degradation of some proteins (alcohol dehydrogenase and αB-crystallin) (21, 22).

Obesity-linked insulin resistance has recently been causally linked to the development of ER stress and an increase in ROS (5, 23, 24). Adipocytes isolated from C57Bl/6J mice with diet-induced obesity have increased reactive oxygen species (25). Oxidative stress in human and murine adipose tissue as well as in cultured 3T3-L1 adipocytes affects the secretion of adipokines such as adiponectin and tumor necrosis factor α (5, 26, 27). As adipokines secreted by adipose tissue have dramatic effects on insulin sensitivity in liver and muscle, determining the effects of oxidative stress in adipose tissue is an important step in understanding the molecular mechanisms of type 2 diabetes and systemic energy metabolism (28). The modification of adipose proteins with lipid peroxidation products could be one contributing factor linking oxidative stress to insulin resistance.

In this study we investigated the modification of adipose proteins by 4-HNE and other aldehydes in lean and obese C57Bl/6J mice. To accomplish this, hydrazide chemistry was used for coupling with aldehyde adducts on proteins (29). Biotin hydrazide tagging allowed evaluation of the relative extent of carbonylation as well as the identification of novel targets of such modifications, including the adipocyte fatty acid-binding protein (A-FABP).

EXPERIMENTAL PROCEDURES

Chemical Reagents—EZ-link biotin hydrazide, FITC-streptavidin, poly-HRP streptavidin, and ImmunoPure Immobilized Monomeric Avidin kit were purchased from Pierce. 4-HNE was purchased from Cayman Chemicals (Ann Arbor, MI). Rabbit anti-4-HNE antibody was purchased from Alpha Diagnostic International (San Antonio, TX). Mouse anti-glutathione *S*-transferase A4 (GSTA4) antibody was purchased from Abnova Corp. (Taipei, Taiwan). Sequencing grade modified trypsin was purchased from Promega. Endoproteinase Glu-C was purchased from Roche Applied Science. 1-Anilinonaphthalene 8-sulfonic acid (1,8-ANS) was purchased from Molecular Probes, Inc. ECL Western blotting detection reagents were purchased from Amersham Biosciences. C_4 and C_{18} Zip Tip pipette tips and YM10 ultrafiltration membranes were purchased from Millipore (Billerica, MA). C_{18} SepPak cartridges were purchased from Waters (Milford, MA). High fat, high carbohydrate diet F3282 was purchased from Bioserve Industries (Frenchtown, NJ). (*R*)-4-HNE and (*S*)-4-HNE were synthesized as described previously (10).

Animals—C57Bl/6J mice were weaned onto high fat or chow diet at 3 weeks of age to induce obesity-linked insulin resistance (30). Using this feeding regimen, at 12 weeks of age the animals exhibit impaired insulin and glucose tolerance as evaluated using glucose and insulin tolerance tests as well as clamping studies (31). The animals were housed on a 12-h light/dark cycle and fed *ad libitum* with continual access to water. The mice were sacrificed by cervical dislocation at 12 weeks of age, and epididymal adipose tissue was recovered. Tissue samples were dissected and stored at −80 °C until needed. The University of Minnesota Institutional Animal Care and Use Committee approved all experiments.

Biotin Hydrazide Modification and Detection—Adipose tissue samples were homogenized in 100 mM sodium acetate, 20 mM NaCl, 0.1 mM EDTA, pH 5.5 (coupling buffer) supplemented with 0.1 mM PMSF, 2 μg/ml pepstatin, 2 μg/ml aprotinin, 2 μg/ml leupeptin. The extract was subjected to centrifugation (100,000 × *g* for 1 h) at 4 °C, the floated lipid cake was removed, and the soluble protein fraction was frozen at −80 °C until needed. Protein concentration was determined using the BCA assay. For aldehyde detection, extracts (50 μg/sample) were incubated with a final concentration of 0.5 mM EZ-link biotin hydrazide (5 mM stock prepared fresh in DMSO) in coupling buffer for 2 h at room temperature, resolved by SDS-PAGE (14% acrylamide), and transferred to PVDF membrane. The membranes were blocked overnight at 4 °C in PBS containing 0.05% Tween 20 (PBST) with 10 mg/ml BSA, washed in PBST, and incubated for 1 h at room temperature with either FITC-conjugated streptavidin (1:50 dilution) or HRP-conjugated streptavidin (1:10,000 dilution). The biotin-avidin interaction was detected using a Fuji imager or by ECL.

For immunodetection of 4-HNE modification of proteins, membranes were blocked in PBST with 10 mg/ml BSA at 4 °C overnight and incubated with anti-4-HNE rabbit polyclonal antibody (1:1,000 dilution) at 4 °C for 16 h in PBST with 1 mg/ml BSA. The membranes were washed in PBST and incubated with HRP-conjugated goat anti-rabbit secondary antibody (1:10,000 dilution) at room temperature for 1 h, and immunoreactivity was detected via ECL. For detection of A-FABP or GSTA4, anti-A-FABP rabbit polyclonal antibody (1:10,000 dilution) or anti-GSTA4 mouse polyclonal antibody (1:2,500) were used for the primary antibody incubation. HRP-conjugated goat anti-mouse secondary antibody (1:10,000 dilution) was used for GSTA4 detection specifically. For both A-FABP and GSTA4 detection, blocking conditions of 10 mg/ml BSA were used throughout the procedures.

Enrichment of Carbonylated Proteins—Soluble adipose tissue protein (10 mg) was incubated with 0.5 mM EZ-link biotin hydrazide in coupling buffer for 2 h at room temperature and dialyzed exhaustively against PBS, pH 7.4, at 4 °C. To remove proteins that bound to Sepharose nonspecifically, the extract was initially passed through a 1-ml column of Sepharose 4B at room temperature, and the flow-through was applied to a monomeric avidin column for 1 h to maximize binding. The column was washed with PBS containing 0.5 M NaCl to remove nonspecifically bound proteins, and specifically bound protein was eluted by the addition of 2 mM D-biotin. The eluted proteins were precipitated with chloroform and methanol, dried under nitrogen, and stored at −20 °C until used (32).

Identification of Carbonylated Proteins by LC-ESI MS/MS—The carbonylated proteins were resolubilized in 250 μl of 50 mM NH_4HCO_3, 1 mM $CaCl_2$, pH 8.5 (trypsin digestion buffer) and digested with 10 μg of trypsin for 15 h at 37 °C. The digestion was stopped by acidification with TFA, and the samples were applied to SepPak C_{18}

cartridges to desalt and remove undigested protein. The peptides were eluted with 80% acetonitrile, 0.1% TFA in water; dried; and reconstituted in 20 μl of 0.1% formic acid.

Analysis of peptides by LC-MS/MS was achieved using the methods described previously (33, 34). Briefly each 20-μl sample was loaded onto a precolumn for concentrating and desalting followed by a C_{18} in-line analytical capillary column (75-μm inner diameter $\times$ 12 cm). The peptides were eluted over a linear gradient of 10–35% acetonitrile in 0.1% formic acid over 60 min at a flow rate of ~250 nl/min followed by isocratic elution at 80% acetonitrile in 0.1% formic acid. Tandem MS analysis of the eluted peptides was performed using either an LCQ classic ion trap mass spectrometer (Finnigan Mat, San Francisco, CA) or an LTQ linear ion trap mass spectrometer system (Thermo Fisher Scientific, Waltham, MA). For each MS survey scan, the top three most abundant precursor ions were selected for MS/MS on the LCQ (33), and the top four most intense precursor ions were selected on the LTQ (34). The instrument settings used for data collection on each platform were identical to those published previously (33, 34), and Xcalibur 2.0 software was used to create the peak lists.

Proteins were identified by analyzing fragment and parent ions using BioWorks 3.2 software and the SEQUEST search algorithm (35) using the International Protein Index (IPI) mouse database, version 3.03 (the database contained 42,402 protein entries at the time it was searched), appended with a reversed database containing reversed sequences of each protein to facilitate false positive rate estimations (36). Oxidation of methionine was included as a variable modification. Mass tolerance was set at 2.0 for parent ions and 1.0 for fragment ions, and trypsin was specified as the enzyme allowing for two internal missed cleavages. Each peptide match was assigned a probability score (*p* score) using the program Peptide Prophet (37). The probability score cutoff value was set at 0.2 for proteins identified from multiple hits (two or more unique peptides) and at 0.90 for single hits. The false positive rate using these thresholds was below 1%, as estimated by reverse database searching, and consistent with our previous studies (38).

Purification of FABPs—Recombinant epithelial fatty acid-binding protein (E-FABP) and A-FABP were expressed in *Escherichia coli* and purified as described previously (39, 40) using a combination of acid and protamine sulfate fractionation followed by gel filtration chromatography using Sephadex G-75. For E-FABP an additional cation exchange chromatography step was utilized. Histidine-tagged A-FABP (His-A-FABP) was expressed in *E. coli* and purified by nickel affinity chromatography and gel filtration chromatography as described previously (41). A-FABP was purified from mouse adipose tissue by methods similar to those described previously for purification from 3T3-L1 adipocytes (42).

Detection of in Vitro 4-HNE Modification by MALDI-TOF MS—Purified E-FABP was incubated with or without 0.5 mM 4-HNE for 20 min at 22 °C in 10 mM potassium phosphate, 150 mM NaCl, pH 7.4 (standard 4-HNE adduction buffer). The reaction was quenched with 100 mM β-mercaptoethanol (βME), and the protein was dialyzed exhaustively to remove excess 4-HNE and βME. C_4 ZipTips were used to desalt the sample, and the presence of a 4-HNE adduct on E-FABP was confirmed by MALDI-TOF MS. For A-FABP, the protein was incubated with 4-HNE in 10 mM potassium phosphate, 10 mM NaCl, pH 7.4 (low salt 4-HNE adduction buffer), and the protein was spotted on a MALDI-TOF target without the use of a ZipTip after the reaction was stopped by acidification with TFA.

MALDI-TOF spectra for undigested proteins were collected as described previously (43). Briefly the samples were spotted with sinapinic acid as the matrix (3,5-dimethoxy-4-hydroxycinnamic acid) in 50:50 acetonitrile:nanopure water, 0.1% TFA. A Bruker Biflex III (Bruker Biosciences, Billerica, MA) equipped with a N_2 laser (337 nm, 3-ns pulse length), and a microchannel plate detector was used to collect data in the linear mode, positive polarity, with an accelerating potential of 19 kV. Each spectrum was obtained by averaging ~200 laser shots. External calibration was performed using singly and doubly charged peaks for horse heart cytochrome *c* (average mass [MH^+], 12,361 Da). The relative amount of protein modified was estimated by dividing the peak intensity for the 4-HNE-modified protein by the sum of the peak intensities for the modified and unmodified protein.

Analysis of the Site of 4-HNE Modification on A-FABP Peptides by MALDI-TOF MS/MS—His-tagged A-FABP was incubated with 4-HNE for 15 h at room temperature in standard 4-HNE adduction buffer. The protein was dialyzed at 4 °C against 25 mM ammonium bicarbonate, pH 8.0. The protein was incubated with 6 M guanidine HCl, 10 mM EDTA, 10 mM DTT for 1 h at 56 °C to denature and reduce the protein. The protein was cooled to room temperature and incubated with iodoacetic acid at a final concentration of 20 mM for 30 min at room temperature in the dark. The protein was dialyzed into trypsin digestion buffer and incubated with trypsin for 15 h at 37 °C or dialyzed against 25 mM sodium phosphate, pH 7.8 (Glu-C digestion buffer) and incubated with Glu-C at room temperature for 15 h. For both enzymes, the ratio of 1:20 protease:protein was used. Digestion was stopped by acidification with TFA. The peptides were desalted with SepPak C_{18} cartridges according to the manufacturer's instructions and spotted with α-cyano-4-hydroxycinnamic acid. Full scans of the peptide mixture from 800 to 3500 *m/z* and tandem mass spectral data of select ions were collected on a QSTAR XL quadrupole time-of-flight mass spectrometer (Applied Biosystems Inc., Foster City, CA). The TOF region acceleration voltage was 4 kV, and the injection pulse repetition rate was 6.0 kHz. Laser pulses were generated with a nitrogen laser at 337 nm, ~9 μJ of laser energy using a laser repetition rate of 20 Hz. Mass spectra were the average of ~50 laser shots collected in positive mode. External calibration was performed daily using human angiotensin II (monoisotopic [MH^+] *m/z*, 1046.5417; Sigma) and adrenocorticotropin hormone fragment 18–39 (monoisotopic [MH^+] *m/z*, 2465.1989; Sigma). Noise was subtracted from MS/MS spectra using the periodic noise filter in Analyst QS, and the centroid peak lists were submitted to Mascot and searched against the National Center for Biotechnology Information non-redundant (NCBInr) (December 1, 2006) *Mus musculus* database (the database contained 107,811 protein entries at the time it was searched) including 4-HNE as a variable modification with mass tolerances set to 0.5 for precursor ions and 0.5 for fragment ions. Centroid peak masses were exported from Analyst QS and graphed using GraphPad Prism software.

Ligand Binding—A-FABP was incubated with and without 0.5 mM 4-HNE at room temperature for 5 h, incubated with 100 mM βME, and dialyzed extensively against 25 mM Tris-HCl, pH. 7.4 (1,8-ANS binding buffer). The 1,8-ANS binding affinity of native and 4-HNE-modified A-FABP was determined by monitoring changes in fluorescence upon titrating the protein into 500 nM 1,8-ANS in 1,8-ANS binding buffer as described previously (44). Excitation and emission wavelengths of 376 and 472 nm, respectively, were used with slit widths of 4 nm for each. Nonlinear regression was carried out using GraphPad Prism software to fit the data to one-site binding isotherms. The isotherm for the 4-HNE-treated protein was modeled as a two-component system to produce a theoretical binding isotherm for the 4-HNE-modified species specifically. Dissociation constant (K_d) values were determined from nonlinear regression.

Statistical Analyses—All values are expressed as mean ± S.E. Statistical significance was determined by performing the two-tailed Student's *t* test assuming unequal variances. *p* values <0.05 are considered significant.

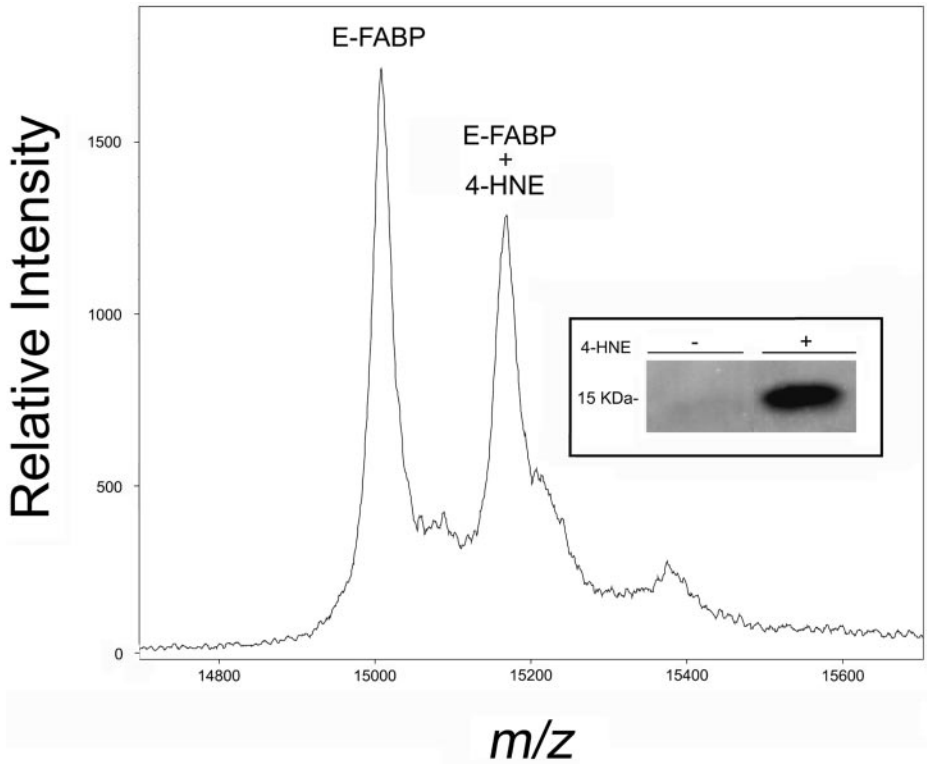

FIG. 1. **Detection of 4-HNE modification of E-FABP.** Purified recombinant mouse E-FABP was incubated with or without 0.5 mM 4-HNE *in vitro*, and the extent of modification was evaluated using MALDI-TOF MS. *Inset*, 10 μg of 4-HNE-modified and unmodified E-FABP were coupled with biotin hydrazide, resolved by SDS-PAGE, transferred to a PVDF membrane, and blotted with FITC-streptavidin.

RESULTS

To assess the relative extent of carbonylation on adipose tissue proteins in lean and obese mice, biotin hydrazide was used as a chemical tag to couple proteins with free carbonyl groups. As an initial means of verifying the ability of biotin hydrazide to detect carbonylated proteins, purified E-FABP, a known target of 4-HNE modification, was evaluated (43). 4-HNE modification was confirmed by the presence of a mass shift of 156 Da when the protein was analyzed by MALDI-TOF MS (Fig. 1). The peak corresponding to a mass of 156 Da larger than that of E-FABP was not detected in the absence of incubation with 4-HNE (Supplemental Fig. 1). After 4-HNE-modified and unmodified E-FABP were incubated with biotin hydrazide, samples were resolved by SDS-PAGE, transferred to PVDF membrane, and incubated with FITC-streptavidin. As shown in Fig. 1, *inset*, biotin hydrazide modified only 4-HNE-modified E-FABP and not the native form.

Using the methods initially developed for detecting 4-HNE modification of E-FABP, soluble adipose protein extracts were coupled with biotin hydrazide, resolved by SDS-PAGE, transferred to membranes, and blotted with HRP-streptavidin. Reaction variables such as biotin hydrazide concentration, temperature, protein amount, and reaction time were altered to optimize the detection of endogenous carbonylation (Supplemental Fig. 2). The reaction was relatively insensitive to temperature or biotin hydrazide concentration but was dependent upon the amount of protein in the reaction. Standard conditions of 0.5 mM biotin hydrazide, 50 μg of protein, 2 h, and 22 °C were chosen for all subsequent biotin hydrazide/HRP-streptavidin blotting experiments. To confirm that biotin hydrazide is highly specific for aldehydes, as has been demonstrated previously for dinitrophenylhydrazine (45), soluble adipose protein was incubated with $NaBH_4$ to reduce aldehydes to primary alcohols. After dialysis, the protein was coupled with biotin hydrazide and blotted with HRP-streptavidin (Supplemental Fig. 3). The signal intensity for the reduced protein was decreased significantly, confirming that the signal intensity from the unreduced protein coupled with biotin hydrazide was primarily from aldehyde groups on the proteins.

To examine the profile of carbonylated proteins in various tissues as well as to confirm that the endogenous carbonylation detected by biotin hydrazide included 4-HNE-modified proteins, soluble protein extracts were prepared from mouse eye, lung, tongue, and adipose tissues. The protein samples were coupled with biotin hydrazide using the standard conditions, resolved by SDS-PAGE, transferred to PVDF membrane, and blotted with HRP-streptavidin. In addition, parallel samples were subjected to immunochemical analysis using an anti-4-HNE antibody. As shown in Fig. 2, different patterns of protein carbonylation were detected in the various tissues, and in general, the profiles of modified proteins were similar, although the biotin hydrazide method appeared to be more sensitive and detected more proteins than did the anti-4-HNE antibody. As hydrazide chemistry has been shown previously to be specific for carbonyl groups (45), the additional bands detected by biotin hydrazide may arise from other carbonyl modifications besides 4-HNE that are known to be prominent

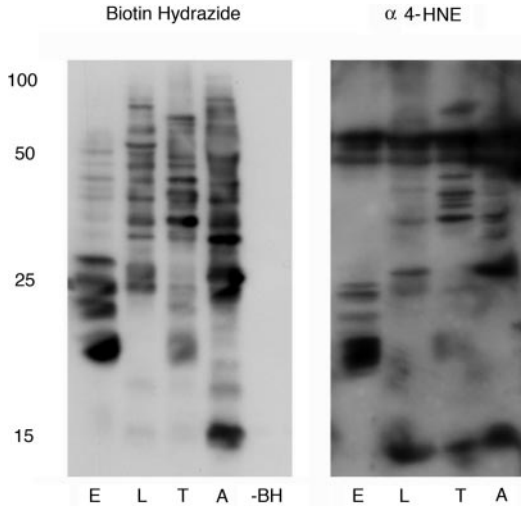

FIG. 2. **Detection of carbonylated proteins in different murine tissues.** Soluble extracts (50 μg) from eye (*E*), lung (*L*), tongue (*T*), or adipose tissue (*A*) were either coupled with biotin hydrazide (using the standard conditions) and detected by blotting with HRP-streptavidin (*left panel*) or immunoblotted with anti-4-HNE antibodies (*right panel*) to detect carbonylated proteins. An additional sample that had not been coupled with biotin hydrazide (−*BH*) was subjected to HRP-streptavidin blotting as a control. Molecular mass (kDa) of protein standards is indicated on the *left*.

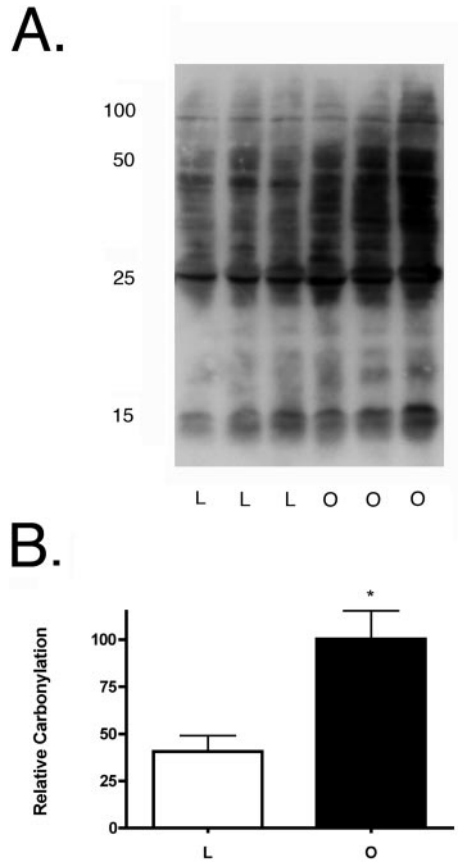

FIG. 3. **Carbonylation of proteins in adipose tissue from lean and obese mice.** *A*, soluble proteins (50 μg) from adipose tissue of lean (*L*) and obese (*O*) mice were coupled with biotin hydrazide, resolved by SDS-PAGE, transferred to PVDF, and blotted with HRP-streptavidin. Molecular masses (kDa) of the proteins are indicated on the *left*. *B*, relative carbonylation (indicated as percentage of the average value for obese mice) was determined from the blot in *A* by densitometry (normalized to total protein). Values are expressed as mean ± S.E. ($n = 3$; *, $p < 0.05$).

(6, 46). Moreover some bands detected by the anti-4-HNE antibody were not observed with the biotin hydrazide method and may be the result of nonspecific reactivity often observed with antibody detection (dark smear at ~55 kDa seen in all samples).

To investigate the extent of carbonylation of proteins in obesity, equal amounts (50 μg) of soluble proteins from epididymal adipose tissue of lean and obese mice were coupled with biotin hydrazide, resolved by SDS-PAGE, transferred to PVDF membrane, and blotted with HRP-streptavidin (Fig. 3*A*). Quantification of signal intensities by densitometry (normalized to total protein) indicated increased ($p < 0.05$) carbonylation of proteins (~2–3-fold) in the samples from the obese mice relative to the lean counterparts (Fig. 3*B*). This finding agrees well with those reported by Talior *et al.* (25) who measured a 2-fold increase in ROS in adipocytes from high fat-fed mice compared with control chow-fed animals. Consistent with increased ROS in adipose tissue of high fat-fed mice, extracts from obese animals exhibited a 3–4-fold decrease ($p < 0.05$) in GSTA4 protein compared with lean animals (Fig. 4). GSTA4 catalyzes the Michael addition of 4-HNE to glutathione (with high specificity for 4-HNE as a substrate), and its decreased abundance may contribute to the increased reactive aldehydes in adipose tissue from high fat-fed mice (47, 48).

To identify proteins that are targets of aldehyde modification, soluble adipose proteins from obese mice were coupled with biotin hydrazide and enriched via affinity chromatography using immobilized monomeric avidin. Bound proteins were eluted with biotin, digested with trypsin, and subjected to LC-ESI MS/MS. Proteins were identified by analyzing parent and fragment ions (Supplemental Fig. 4) using SEQUEST. All data were filtered using the SEQUEST parameters described under "Experimental Procedures." The experiment was performed multiple times and repeated in the absence of biotin hydrazide coupling to control for nonspecific enrichment by the avidin column. After removing all proteins that were enriched without biotin hydrazide coupling, a list of soluble proteins identified as targets of aldehyde modification in adipose tissue was generated (Table I). Peptides matched to keratins, serum proteins, trypsin, and hypothetical proteins were also removed from the list. The identified proteins sorted into the following clusters: carbohydrate and lipid metabolism, signal transduction, antioxidant enzymes/cell stress response, nucleic acid metabolism, protein synthesis/degradation, and structural/motor proteins. Of particular note was A-FABP/aP2, a cytoplasmic fatty acid carrier protein and a

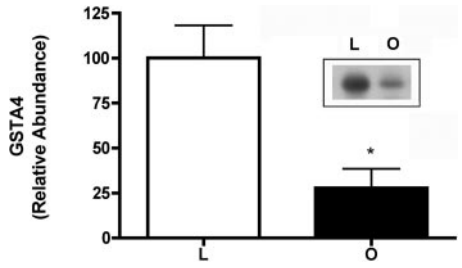

FIG. 4. **Protein levels of GSTA4 in lean and obese mice.** Soluble protein (50 μg) from adipose tissue of lean and obese mice was resolved by SDS-PAGE, transferred to PVDF, and immunoblotted with anti-GSTA4 antibody. Relative abundance (indicated as percentage of the average value for lean mice) was determined by densitometry (normalized to total protein). Values are expressed as mean ± S.E. ($n = 8$; *, $p < 0.05$). *Inset*, representative lean (*L*) and obese (*O*) samples from anti-GSTA4 immunoblot.

member of the multigene family of lipid-binding proteins that includes previously characterized E-FABP (43).

Because A-FABP was found to be an *in vivo* target of aldehyde modification in adipose tissue by LC-ESI MS/MS, adipose extracts from A-FABP-null mice were used to confirm that A-FABP was modified with 4-HNE (Fig. 5). When soluble adipose protein extracts from wild type mice were subjected to aldehyde detection via biotin hydrazide coupling/HRP-streptavidin blotting, a prominently modified protein was detected at ~15 kDa that was absent in protein extracts from A-FABP-null mice. When these same samples were subjected to immunoblotting with an anti-4-HNE antibody a similar result was observed. To further verify that A-FABP is a target of 4-HNE modification *in vivo*, the protein was purified from mouse adipose tissue. Both biotin hydrazide/streptavidin blotting and immunoblotting with anti-4-HNE antibody confirmed that A-FABP was modified with 4-HNE *in vivo* (Fig. 5).

To determine the stoichiometry of *in vivo* 4-HNE modification of A-FABP, quantitative immunoblotting using antibodies directed to 4-HNE and A-FABP was utilized (Supplemental Fig. 5). The fraction of A-FABP modified with 4-HNE in adipose tissue of obese mice was calculated by determining the concentrations of total A-FABP and 4-HNE-modified A-FABP in tissue extracts. Through immunodetection of either A-FABP or 4-HNE-modified A-FABP, it was estimated that 6–8% of total A-FABP is modified by 4-HNE in adipose tissue of obese mice. Given the total abundance of A-FABP is ~250 μM in adipocytes (42), the concentration of 4-HNE-modified protein was estimated to be 15–20 μM.

To further characterize the modification of A-FABP with 4-HNE, purified protein was incubated with 0.5 mM (*R*)- or (*S*)-4-HNE or a 50:50 racemic mixture for various lengths of time, and the extent of modification was assessed using MALDI-TOF mass spectrometry (linear mode). As shown in Fig. 6, there was no statistical difference between the extent of modification of the protein by (*R*)- or (*S*)-4-HNE compared with the racemic mixture.

To identify the site of 4-HNE modification of A-FABP *in vitro*, His_6-tagged A-FABP was incubated with 4-HNE and enzymatically digested with either trypsin or Glu-C, and the resulting peptides were subjected to MALDI-TOF MS/MS analysis (41). The *m/z* values of abundant ions in the initial MS spectra demonstrated A-FABP sequence coverage of 47.7% for Glu-C and 73.5% for trypsin (data not shown). For both trypsin and Glu-C digestions, parent ions with *m/z* values corresponding to a peptide with Cys-117 modified by 4-HNE (1076.5 for trypsin and 1628.8 for Glu-C) were isolated and subjected to fragmentation to generate MS/MS spectra (Fig. 7). Many of the ions in the MS/MS spectra observed corresponded to those in the predicted fragmentation pattern for the peptides with Cys-117 modified by 4-HNE (Table II). The 4-HNE modification itself appeared to undergo significant neutral loss fragmentation during the collision-induced dissociation process (labeled as $[M + H]^{+1} - 156$ for parent ion and with * for fragment ions in Fig. 7), a commonly observed event during MS/MS analysis of 4-HNE-modified peptides (49, 50) resulting in parent and fragment ions with 4-HNE modification intact in some cases and absent in others. The presence of *b* ions at 104.0 and 260.1 *m/z* in the spectrum for the Glu-C-digested peptide (Fig. 7*A*, labeled as *b1* and *b1**) verify that the 4-HNE modification is on Cys-117 as these *m/z* values correspond to N-terminal *b1* ions consisting only of cysteine with and without the addition of 4-HNE. The 104.0 *m/z* peak represents the unmodified Cys-117 with the 260.1 *m/z* peak representing the same cysteine with the 4-HNE modification intact, giving it an additional 156 *m/z* units. Furthermore the additional 156 *m/z* units was only seen on *b* ions for the tryptic peptide in which Cys-117 is part of the given fragment (ions indicative of 4-HNE modification at Cys-117 are shown in bold in Table II). No fragments besides those containing Cys-117 were found to have 4-HNE adducts, and no other 4-HNE-modified peptides were detected for either digest. A-FABP contains no histidine residues and only one additional cysteine, Cys-1, making it the only other strong candidate as a potential site of *in vitro* 4-HNE modification. Although ions with *m/z* values corresponding to peptides with Cys-1 in the unmodified (alkylated with iodoacetic acid) state were detected for both trypsin and Glu-C, the corresponding ion for a 4-HNE-modified peptide was absent in each case. The reactivity of lysine with 4-HNE is much weaker than that of cysteine or histidine, and we found no evidence for a lysine modification on A-FABP at a detectable level. Furthermore the MS/MS spectra in Fig. 7 were submitted to Mascot to search against the mouse database in an unbiased way using 4-HNE as a variable modification. For both the trypsin and Glu-C digests, the Cys-117 HNE-modified peptide derived from A-FABP was the top scoring sequence match with Molecular Weight Search scores of 14 for trypsin and 39 for Glu-C (where a Molecular Weight Search score of greater than 32 indicates identity or extensive homology at $p < 0.05$) (51). Together this evidence demonstrates that Cys-117 is the site of 4-HNE modification on A-FABP *in vitro*.

TABLE I

Identification of carbonylated proteins in adipose tissue

Soluble proteins from adipose tissue of obese mice were coupled with biotin hydrazide, enriched *via* affinity chromatography using immobilized monomeric avidin, and digested with trypsin. Peptides were subjected to LC-ESI MS/MS, and proteins were identified using SEQUEST software. The identified proteins are listed along with their accession number. The peptides sequenced for each protein are indicated along with the Peptide Prophet probability score (P score), the charge of the peptide (*z*), the singly charged mass ($[M + H]^{+1}$) with the experimental error shown in parentheses, the cross-correlation value (Xcor), delta correlation value (Δcor), and preliminary score rank (Rsp).

Protein Name / Peptide	Accession # / P score	*z*	$[M+H]^{+1}$ (error)	Xcor	Δcor	Rsp
Carbohydrate and Lipid Metabolism						
Fatty acid synthase	**NP: NP_032014**					
K.GVDLVLNSLAEEK.L	0.3863	2	1387.6 (+0.0)	1.8524	0.112	1
R.LLLPEDPLISGLLNSQALK.A	1.0000	2	2035.4 (-0.4)	3.2757	0.531	1
Fatty acid binding protein 4, adipocyte	**NP: NP_077717**					
K.LVSSENFDDYMK.E	0.9981	2	1448.6 (-0.2)	3.145	0.475	1
Triosephosphate isomerase 1	**NP: NP_033441**					
K.VTNGAFTGEISPGMIK.D	0.9619	2	1622.9 (+0.8)	2.7953	0.348	1
UDP-N-acteylglucosamine pyrophosphorylase 1-like 1 protein	**NP: NP_001028465**					
R.AALLAELASLEADALR.E	0.9851	2	1627.9 (+0.4)	3.2037	0.382	1
K.FVFDVFQFAK.N	0.9894	2	1248.5 (-0.5)	2.1232	0.421	1
Glyceraldehyde 3-phosphate dehydrogenase	**NP: NP_001001303**					
R.VIISAPSADAPMFVMGVNHEK.Y	0.9933	2	2214.6 (+1.2)	4.0324	0.528	1
Fumarate hydratase 1	**NP: NP_034339**					
K.ETAIELGYLTAEQFDEWVKPK.D	1.0000	2	2468.7 (+1.6)	4.5398	0.514	1
R.MPIPVIQAFGILK.R	0.9354	2	1427.8 (-0.2)	2.1817	0.281	1
β enolase	**SWISS-PROT: P21550**					
K.LAQSNGWGVMVSHR.S	0.9852	2	1542.7 (+0.8)	3.1848	0.377	1
Signal Transduction						
Ubiquitin-activating enzyme E1-domain containing 1 protein	**NP: NP_079968**					
R.IQEMSDEVLDSNPYSR.L	0.9990	2	1884.0 (+0.5)	3.7034	0.522	1
A kinase (PRKA) anchor protein (gravin) 12	**NP: NP_112462**					
K.KDEGEGAEASVGAGDHQEPGVETVGESASK.E	0.9989	3	2929.0 (-1.2)	3.7528	0.551	1
Protein-tyrosine phosphatase, receptor-type, S	**NP: NP_035348**					
R.NVLELTDVK.D	0.9421	2	1031.2 (+1.1)	2.2163	0.323	1
Myotubularin-related protein 2	**NP: NP_076347**					
R.EANKLAEMEEPALLPGENIKDM*AK.D	0.9114	3	2659.0 (-0.4)	2.3467	0.409	1
Gelsolin	**NP: NP_666232**					
R.VPFDAATLHTSTAMAAQHGMDDDGTGQK.Q	0.9994	3	2875.1 (-0.6)	6.6707	0.658	1
Filamin A	**SWISS-PROT: Q8BTM8**					
K.KTHIQDNHDGTYTVAYVPDVPGR.Y	0.9344	3	2584.8 (-0.3)	2.3312	0.350	1
R.LIALLEVLSQK.K	0.5076	2	1227.5 (+1.7)	1.6623	0.356	5
Galectin-3	**SWISS-PROT: P16110**					
K.IQVLVEADHFK.V	0.9757	2	1299.5 (-0.0)	2.8569	0.281	1
Antioxidant Enzymes / Cell Stress Response						
Peroxiredoxin 1	**NP: NP_035164**					
R.LVQAFQFTDK.H	0.9964	2	1197.4 (+0.1)	2.6647	0.439	1
K.PGSDTIKPDVNK.S	0.7582	3	1271.4 (+0.7)	3.1026	0.298	1
R.TIAQDYGVLK.A	0.9480	2	1108.3 (-0.1)	2.1014	0.289	1
K.QGGLGPMNIPLISDPK.R	0.9964	2	1637.9 (-0.1)	3.2269	0.490	1
Glutathione peroxidase 1	**NP: NP_032186**					
R.NALPTPSDDPTALMTDPK.Y	0.9933	2	1885.1 (-0.5)	2.9583	0.474	1
Glutathione S-transferase M1	**NP: NP_034488**					
R.KHHLDGETEEER.I	0.9853	3	1480.5 (+0.8)	3.392	0.341	1
Aldehyde dehydrogenase family 6, subfamily A1	**NP: NP_598803**					
K.WIDIHNPATNEVVGR.V	0.9952	2	1721.9 (+1.3)	2.9254	0.491	1
R.VNAGDQPGADLGPLITPQAK.E	0.8867	2	1963.2 (-0.5)	2.5988	0.473	1
Aldehyde dehydrogenase family 1, subfamily A7	**NP: NP_036051**					
R.ELGEHGLYEYTELK.T	0.9357	2	1681.8 (-0.7)	2.5294	0.375	1
K.IHGQTIPSDGNIFTYTR.R	0.9883	2	1921.1 (-1.0)	3.2252	0.460	1
K.VSFTGSTEVGK.L	0.6075	2	1112.2 (-0.4)	1.8341	0.189	2
K.IFINNEWHDSVSSK.K	0.9914	2	1676.8 (-0.3)	3.1566	0.322	1
Aldehyde dehydrogenase 1 family, member L1	**NP: NP_081682**					
R.ILPNVPEVEDSTDFFK.S	0.9540	2	1851.0 (+0.2)	2.4273	0.282	1
Vacuolar ATP synthase subunit B, isoform2	**NP: NP_031535**					
R.IYPEEMIQTGISAIDGMNSIAR.G	0.9533	2	2410.8 (+1.7)	2.8575	0.360	1
Calumenin	**NP: NP_031620**					
K.VHNDAQNFDYDHDAFLGAEEAK.S	0.9627	3	2507.6 (+2.0)	5.1898	0.553	1

TABLE I— *continued*

Protein Name / Peptide	Accession # / P score	z	[M+H]$^{+1}$ (error)	Xcor	Δcor	Rsp
Nucleic Acid Metabolism						
Dihydropyrimidinase related protein-2	**SWISS-PROT: O08553**					
K.AALAGGTTMIIDHVVPEPGTSLLAAFDQWR.E	1.0000	2	3139.6 (+0.2)	3.8491	0.592	1
K.GTVVYGEPITASLGTDGSHYWSK.N	0.8989	2	2426.6 (+0.4)	2.0676	0.353	1
K.IVLEDGTLHVTEGSGR.Y	0.9968	2	1683.8 (+0.5)	3.9131	0.559	1
K.MDENQFVAVTSTNAAK.V	0.9638	2	1726.9 (-0.6)	2.376	0.312	1
R.FQLTDSQIYEVLSVIR.D	0.9915	2	1912.2 (-0.2)	3.4469	0.451	1
Damage specific DNA binding protein 1	**NP: NP_056550**					
R.IEVQDSSGGTTALRPSASTQALSSSVSSSK.L	0.9890	3	2940.1 (+0.1)	4.0238	0.523	1
K.ICYQEVSQCFGVLSSR.I	0.6283	2	1820.1 (+0.5)	2.1314	0.247	3
Seryl-aminoacyl-tRNA synthetase 1	**NP: NP_035449**					
K.EAVGDDESVPENVLNFDDLTADALAALK.V	0.9437	2	2933.1 (-0.6)	1.949	0.347	1
Step II Splicing factor SLU7 homolog	**TREMBL: Q6P923**					
K.DHNSEDEDEDK.Y	0.9649	2	1333.2 (+0.2)	2.1669	0.319	1
Protein Synthesis / Degradation						
Eukaryotic translation elongation factor 1 β 2	**NP: NP_061266**					
K.TPAGLQVLNDYLADK.S	0.9888	2	1618.8 (-0.8)	3.2266	0.503	1
Eukaryotic translation elongation factor 1 α 1	**NP: NP_034236**					
K.RYEEIVK.E	0.8050	2	937.1 (+0.4)	2.542	0.136	2
K.YYVTIIDAPGHR.D	0.9581	2	1405.6 (+1.0)	3.1618	0.309	1
Serine (or cysteine) proteinase inhibitor, clade A, member 1a	**NP: NP_033269**					
K.DQSPASHEIATNLGDFAISLYR.E	0.9992	2	2406.6 (+0.3)	3.5043	0.486	1
Structural / Motor Proteins						
Myosin, heavy polypeptide 6, cardiac muscle, α	**NP: NP_034986**					
R.DLEEATLQHEATAAALR.K	0.9985	2	1840.0 (-0.3)	4.3808	0.582	1
R.IEELEEELEAER.T	0.5393	2	1489.6 (-0.4)	2.8021	0.174	1
K.LEQQVDDLEGSLEQEK.K	0.9935	2	1861.0 (-0.4)	3.6673	0.458	1
K.NLTEEMAGLDEIIAK.L	0.2056	2	1647.9 (+1.6)	3.2268	0.532	2
K.HADSVAELGEQIDNLQR.V	0.9998	2	1896.0 (-0.6)	3.8176	0.528	1
Myosin light chain, phosphorylatable, fast skeletal muscle	**NP: NP_058034**					
K.GADPEDVITGAFK.V	0.9224	2	1320.4 (+0.1)	1.912	0.318	1
Myosin, heavy polypeptide 8, skeletal muscle, perinatal	**NP: NP_796343**					
R.AEDEEEINAELTAK.K	0.9988	2	1562.6 (-0.1)	3.6427	0.519	1
K.VLNASAIPEGQFIDSK.K	0.5253	2	1689.9 (-0.5)	1.645	0.227	2
R.VQLLHTQNTSLINTK.K	0.9987	2	1711.0 (-0.2)	3.4139	0.471	1
K.TPGAMEHELVLHQLR.C	0.9788	3	1732.0 (+0.3)	4.3845	0.483	1
Myosin, heavy polypeptide 2, skeletal muscle, adult	**NP: NP_659210**					
R.LEEAGGATSAQIEMNK.K	0.9700	2	1649.8 (+0.1)	2.0632	0.377	1
R.LQNEVEDLMLDVER.T	0.5262	5	1703.9 (-0.5)	2.8203	0.449	1
Myosin, heavy polypeptide 4, skeletal muscle	**NP: NP_034985**					
K.YEETQAELEASQK.E	0.9991	2	1526.6 (-0.6)	3.647	0.585	1
R.VAEQELLDASER.V	0.9957	2	1360.5 (-0.4)	2.6462	0.436	1
Cofilin 1, non-muscle	**NP: NP_031713**					
K.LGGSAVISLEGK.P	0.9984	2	1131.3 (+0.2)	4.174	0.515	1
Cofilin 2, muscle	**NP: NP_031714**					
R.YALYDATYETK.E	0.9986	2	1338.4 (+0.2)	2.872	0.481	1
Destrin	**NP: NP_062745**					
K.EILVGDVGATITDPFK.H	1.0000	1	1675.9 (-0.3)	3.2593	0.494	1
R.YALYDASFETK.E	0.9994	2	1308.4 (+1.1)	3.2691	0.485	1

*	Oxidized methionine residue.
.	Trypsin cleavage site.
[M+H]$^{+1}$	Calculated, average masses for the identified peptide sequence.
(error)	Difference between [M+H]$^{+1}$ for the identified peptide sequence and the measured value based on the mass of the ion selected for MS/MS.

To verify that Cys-117 is the *in vivo* site of modification (and in agreement with the reactivity of the protein with 4-HNE *in vitro*), A-FABP purified from mouse adipose tissue was digested with Glu-C and subjected to MALDI-TOF MS. The spectrum obtained had 67.9% sequence coverage for A-FABP. Peaks at 1641.8 and 1530.6 *m/z* were detected, cor-

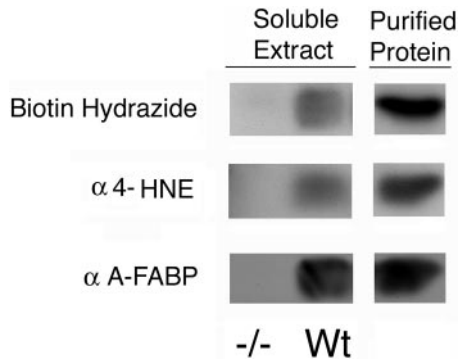

FIG. 5. ***In vivo* carbonylation and 4-HNE modification of A-FABP.** *Left*, soluble protein (50 μg) from adipose tissue of A-FABP null (−/−) and wild type (*Wt*) mice was evaluated using either biotin hydrazide coupling or immunochemically using anti-4-HNE and anti-A-FABP antiserum. *Right*, A-FABP was purified from murine adipose tissue and subjected to a parallel analysis.

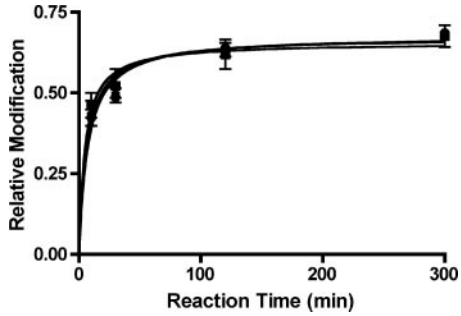

FIG. 6. ***In vitro* modification of A-FABP by 4-HNE enantiomers.** Purified A-FABP was incubated with 0.5 mM (*R*)-4-HNE, (*S*)-4-HNE, or a 50:50 racemic mixture. After various time points, the protein was subjected to MALDI-TOF MS analysis. The relative extent of 4-HNE modification was estimated from spectral peak intensities. The experiment was done in triplicate with *error bars* shown. *Squares* represent (*R*)-4-HNE, *circles* represent (*S*)-4-HNE, and *diamonds* indicate 50:50 racemic mixture.

responding to unmodified peptides containing Cys-1 (acetylated) and Cys-117 alkylated with iodoacetic acid. Although no peak was observed corresponding to a peptide with Cys-1 modified with 4-HNE or 4-ONE, a cluster of peaks at 1626.6, 1627.6, and 1628.6 *m/z* (signal:noise between 4 and 5 for each peak) was observed (Supplemental Fig. 6) and is in agreement with the theoretical monoisotopic *m/z* values of the predicted Glu-C peptide with Cys-117 modified with 4-ONE (1626.8) and 4-HNE (1628.8). Although it is unclear whether the 1628.6 *m/z* peak is part of the isotope envelope for a monoisotopic peak at 1626.6 *m/z* (as the 1627.6 peak likely is) or whether it is the result of an independent modification, these *m/z* values are in agreement with the modified Glu-C peptide observed in the *in vitro* studies (Table II). In addition, this peak cluster was absent in a control Glu-C digest of *E. coli*-expressed recombinant A-FABP, which had 74.0% sequence coverage for A-FABP and contained the peak corresponding to the peptide with Cys-117 alkylated with iodoacetic acid (data not shown).

To investigate the effect of 4-HNE modification of A-FABP on its fatty acid binding activity, recombinant protein was modified with 4-HNE, and the binding of the surrogate fluorescent ligand 1,8-ANS was monitored (44). Fig. 8 shows the binding isotherm for the native and 4-HNE-modified protein with native A-FABP exhibiting a K_d of 2.05 ± 0.17 μM and the 4-HNE-modified A-FABP exhibiting a K_d of 23.20 ± 4.18 μM ($p < 0.05$).

DISCUSSION

Obesity and type 2 diabetes are correlated with an increase in ER stress (5, 23) and increased ROS (5, 23). One possible contributing factor of obesity to insulin resistance is oxidative stress-induced lipid peroxidation and the modification of proteins by reactive aldehydes such as 4-HNE and 4-ONE. To gain insight into the extent of carbonylation of adipose proteins, biotin hydrazide was used as an affinity tag for proteins with free aldehyde groups (29). Whereas other studies have demonstrated an increase in oxidative stress markers such as malondialdehyde and ROS measurements (5, 25), to our knowledge this is the first report of direct protein modification in adipose tissue linked to obesity. The ~2–3-fold increase in protein carbonylation accompanying high fat feeding agrees with other measures of oxidative stress (25). In addition, 37 targets of aldehyde modification were identified in adipose tissue of the obese mice.

Several proteins we identified in this study have been reported previously to be carbonylated or 4-HNE-modified specifically in other systems. Glyceraldehyde-3-phosphate dehydrogenase and glutathione *S*-transferase M1 have been shown to be targets of 4-HNE (52). In addition, dihydropyrimidinase-related protein 2 has been shown to be carbonylated in brain of Alzheimer disease patients, and triose-phosphate isomerase 1 has been found to be carbonylated in yeast upon treatment with hydrogen peroxide (53). As we found similarities between the detection of proteins with biotin hydrazide and anti-4-HNE antibody in adipose and other tissues, we presume that many of the proteins identified by enrichment via biotin hydrazide coupling are 4-HNE-modified (Fig. 2). However, as amino acid side chain oxidation and other lipid peroxidation products can also result in aldehyde groups on proteins (6, 46), additional studies need to be done to confirm the type of modification present on each specific protein of interest as we have done for A-FABP.

Work from this laboratory has shown previously that E-FABP is a target of 4-HNE modification in retina and that the site of modification is Cys-120 (corresponding to Cys-117 in A-FABP) (43). A-FABP and E-FABP are members of the intracellular fatty acid-binding protein multigene family, share ~60% amino acid identity, and have essentially superimposable secondary and tertiary structures (54, 55). The defining feature of the FABP multigene family is a large interior water-filled cavity that serves as the hydrophobic ligand-binding domain. Lipid binding to A-FABP occurs within a defined fatty acid binding site with the carboxyl group coordinated by

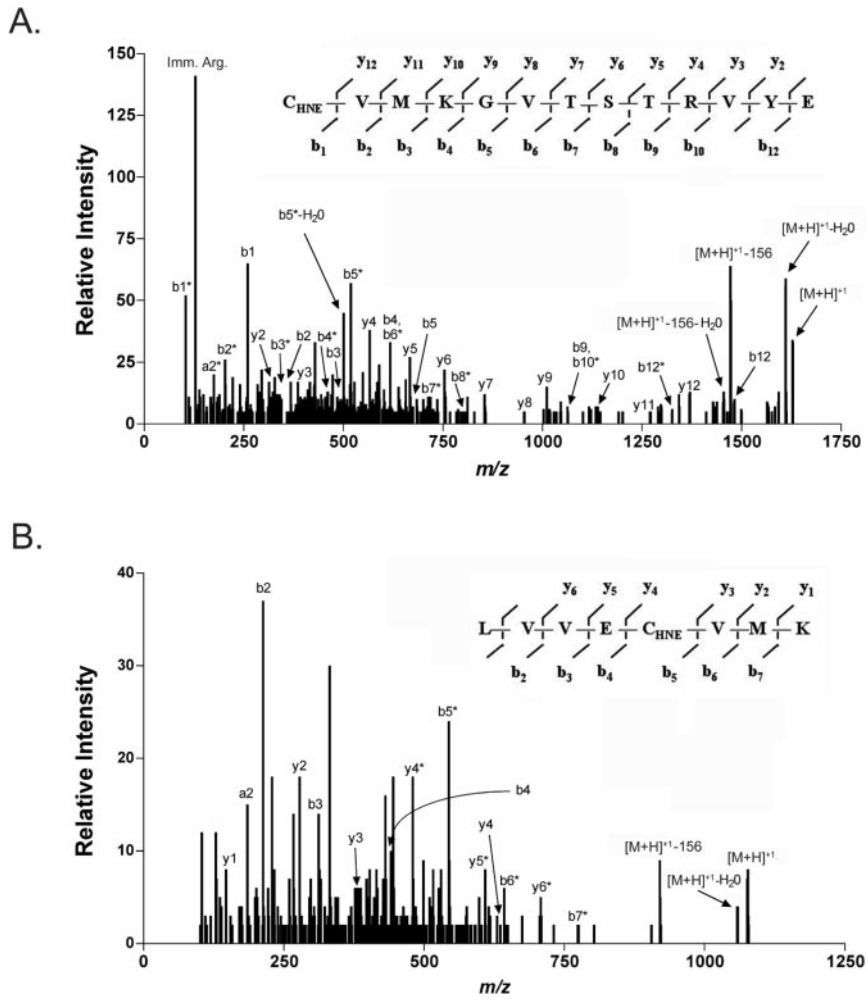

FIG. 7. **MS/MS spectra of 4-HNE-modified A-FABP peptides.** A-FABP was modified with 0.5 mM 4-HNE *in vitro* and digested with either Glu-C protease (*A*) or trypsin (*B*). In each case, the ion with *m/z* corresponding to the predicted 4-HNE-modified peptide was isolated and subjected to fragmentation. Both the $[M + H]^{+1}$ parent ion peak corresponding to the 4-HNE-modified peptide as well as the peak corresponding to the neutral loss of 4-HNE ($[M + H]^{+1} - 156$) are labeled. The *b* and *y* ions observed are labeled as well as several observed *a* ions, an immonium ion of an arginine residue (*Imm. Arg.*), and ions corresponding to the loss of water ($-H_2O$). Fragment ions demonstrating neutral loss of 4-HNE are indicated with an *asterisk* (*).

Arg-106, Arg-126, and Tyr-128 (56). The decreased binding affinity of 4-HNE-modified A-FABP for the hydrophobic probe 1,8-ANS (Fig. 8) agrees with the finding of Cys-117 as the site of modification (Fig. 7) and is consistent with a variety of crystallographic and NMR studies on the A-FABP apo- and holoprotein forms. X-ray crystallographic analysis of A-FABP in a variety of fatty acid-bound forms (palmitate, stearate, and arachidonate) have shown that the C_3 to C_6 region of a bound lipid lies in close proximity to Cys-117 (57–59). Moreover chemical modification of Cys-117 *in vitro* with a battery of sulfhydryl reagents decreased the affinity of A-FABP for fatty acids, and fatty acid binding attenuated Cys-117 modification (60). Prior to this study, only long and very long chain fatty acids were believed to bind within the cavity (44). This report implies that the ligand binding specificity of FABPs is broader than previously considered and extends to medium chain aldehydes. It will be interesting in the future to determine whether testis FABP, which exhibits the same structurally conserved cysteine residue, is also 4-HNE-modified.

The presence of a cluster of peaks containing ions with *m/z* 1626.6 and 1628.6 in the MALDI-TOF MS spectrum of *in vivo* purified A-FABP digested with Glu-C (Supplemental Fig. 6) is consistent with the finding of Cys-117 as the *in vitro* site of modification (Fig. 7). As further support for *in vivo* modification at Cys-117, digestion of recombinant *E. coli*-derived A-FABP (*E. coli* lacks large amounts of polyunsaturated fatty acid substrates for 4-ONE and 4-HNE synthesis) revealed no peak cluster at these *m/z* values. It is not surprising that a significant portion of the modified species of A-FABP *in vivo* may be alkylated with 4-ONE (consistent with 1626.6 peak) at Cys-117 in addition to 4-HNE (consistent with 1628.6 peak). Because 4-ONE contains a more electronegative keto function relative to the hydroxyl group of 4-HNE it has been measured to be significantly more reactive than 4-HNE (61).

It has been shown previously that A-FABP has a role in insulin resistance in mice (31), and A-FABP-null mice are relatively insulin-sensitive compared with wild type C57Bl/6J littermates. In light of this, covalent binding of 4-HNE may promote the holoprotein structure, mimicking the fatty acid-bound state. As the interaction of A-FABP and hormone-sensitive lipase has been shown previously to be fatty acid-dependent (41), the level at which A-FABP is modified with 4-HNE could have significant effects on lipolysis in the adipocyte. In this study it was estimated that 6–8% of A-FABP is modified with 4-HNE in adipose

TABLE II

Ions observed in MS/MS fragmentation of 4-HNE-modified A-FABP peptides

Ions with *m/z* corresponding to predicted 4-HNE-modified A-FABP peptides were isolated and fragmented using an Applied Biosystems QSTAR XL instrument. The observed MS/MS ions agree with theoretical fragmentation patterns for an A-FABP peptide modified on Cys-117, generated by digestion with both trypsin and Glu-C. Peptide fragments indicative of cysteine modification with 4-HNE are indicated in bold.

Enzyme: Glu-C — *m/z* of isolated ion: 1628.8

Precursor peptide	Theoretical $[M+H]^{+1}$ - 4-HNE	Theoretical $[M+H]^{+1}$ + 4-HNE	Observed $[M+H]^{+1}$	Observed $[M+H]^{+1}$ + 156
$C_{(HNE)}$VMKGVTSTRVYE	1472.7	1628.8	1472.7	**1628.8**

Terminal Residue	Theoretical *b* ions - 4-HNE	Theoretical *b* ions + 4-HNE	Observed $[M+H]^{+1}$ - 4-HNE	Observed $[M+H]^{+1}$ + 4-HNE	Theoretical *y* ions - 4-HNE	Theoretical *y* ions + 4-HNE	Observed $[M+H]^{+1}$ - 4-HNE	Observed $[M+H]^{+1}$ + 4-HNE
Cys 117/HNE	104.0	260.1	104.0	**260.1**	-	-	-	
Val 118	203.1	359.2	203.1	**359.2**	1369.7	NA	1369.7	
Met 119	334.1	490.2	334.1	**490.2**	1270.6	NA	1270.6	
Lys 120	462.2	618.3	462.2	**618.3**	1139.6	NA	1139.6	
Gly 121	519.2	675.4	519.2	**675.3**	1011.5	NA	1011.5	
Val 122	618.3	774.4	618.3		954.5	NA	954.5	
Thr 123	719.4	875.5	719.3		855.4	NA	855.4	
Ser 124	806.4	962.5	806.4		754.4	NA	754.3	
Thr 125	907.4	1063.6		**1063.5**	667.3	NA	667.3	
Arg 126	1063.5	1219.7	1063.5		566.3	NA	566.3	
Val 127	1162.6	1318.7			410.2	NA	410.2	
Tyr 128	1325.7	1481.8	1325.7	**1481.7**	311.1	NA	311.1	
Glu 129	1454.7	1610.8	1454.7	**1610.8**	148.1	NA		

Enzyme: Trypsin — *m/z* of isolated ion: 1076.5

Precursor Peptide	Theoretical $[M+H]^{+1}$ - 4-HNE	Theoretical $[M+H]^{+1}$ + 4-HNE	Observed $[M+H]^{+1}$	Observed $[M+H]^{+1}$ + 156
LVVE$C_{(HNE)}$VMK	920.5	1076.6	920.5	**1076.5**

Terminal Residue	Theoretical *b* ions - 4-HNE	Theoretical *b* ions + 4-HNE	Observed $[M+H]^{+1}$ - 4-HNE	Observed $[M+H]^{+1}$ + 4-HNE	Theoretical *y* ions - 4-HNE	Theoretical *y* ions + 4-HNE	Observed $[M+H]^{+1}$ - 4-HNE	Observed $[M+H]^{+1}$ + 4-HNE
Lue 113	114.1	NA			-	-	-	
Val 114	213.2	NA	213.2		807.4	936.5		
Val 115	312.2	NA	312.2		708.3	864.5	708.3	
Glu 116	441.3	NA	441.3		609.3	765.4	609.3	
Cys 117/HNE	544.3	700.4	544.3		480.2	636.3	480.2	**636.3**
Val 118	643.3	799.5	643.3		377.2	NA	377.2	
Met 119	774.4	930.5	774.3		278.2	NA	278.2	
Lys 120	902.5	1058.6		**1058.5**	147.1	NA	147.1	

tissue of obese mice. Because of the high level of expression of A-FABP in adipose tissue (250 μM), this seemingly modest fraction that is modified would accumulate to relatively high concentration (15–20 μM HNE-modified A-FABP) in obese mice. The relative extents of modification of A-FABP in lean and obese mice was consistent with the ~2–3-fold increase in total protein carbonylation (Fig. 3), and increased modification of A-FABP may in part contribute to insulin resistance in obesity through altering hormone-sensitive lipase activity.

A potential role for A-FABP is as an antioxidant protein, scavenging 4-HNE in the cell (43). Glutathione, a well characterized antioxidant against 4-HNE, has been shown to be enantioselective toward (*S*)-4-HNE in its GST-catalyzed Michael adduct formation (62). The fact that A-FABP forms adducts with both enantiomers of 4-HNE suggests that such a 4-HNE-scavenging role would not be completely overlapping with that of glutathione. As both stereoisomers of 4-HNE are formed in the cell, the ability of FABP to form adducts with (*R*)-4-HNE could be an important way of regulating concentrations of free 4-HNE.

Several other proteins identified in this study as targets of

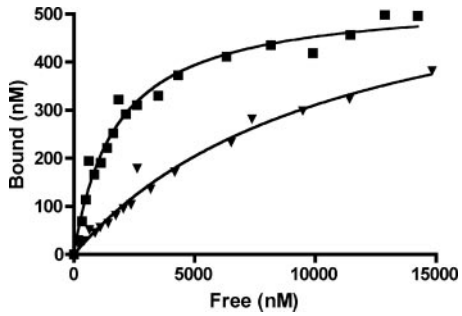

FIG. 8. **Effect of 4-HNE modification of A-FABP on 1,8-ANS binding.** After modification with or without 0.5 mM 4-HNE, A-FABP was titrated into 1,8-ANS, and the binding isotherm was calculated from monitoring changes in fluorescence. The experiment was done in triplicate, and the results shown are representative of the three trials. *Squares* represent untreated A-FABP, and *triangles* represent 4-HNE-modified A-FABP.

carbonylation may contribute to insulin resistance and inflammation. The well characterized roles of peroxiredoxin 1 and glutathione peroxidase 1 are in reducing hydroperoxides in the cell, including lipid hydroperoxides (63, 64). However, peroxiredoxin and glutathione peroxidase enzymes have also been shown to be important for the regulation of signal transduction pathways through controlling the redox state of proteins and lipids. Specifically the nuclear localization of NFκB, a stress-activated transcription factor known to contribute to insulin resistance in adipose tissue through the control of adipokine expression, has been shown to be negatively regulated in part by peroxiredoxin and glutathione peroxidase proteins (65–67). Furthermore the presence of active site cysteine (peroxiredoxin 1) and selenocysteine (glutathione peroxidase) residues makes these enzymes strong candidates for being inactivated by alkylation with 4-HNE, which could play a role in activating the NFκB stress response in obesity. In addition, glutathione *S*-transferase and aldehyde dehydrogenase family members are important antioxidants against 4-HNE and other electrophilic lipids (6). Their potential inactivation through modification could contribute to cellular stress by amplifying oxidative stress in obesity.

The actin filament-binding protein filamin A has been shown to interact with the insulin receptor and inhibit insulin signal transduction (68). The modification of filamin A with a lipid such as 4-HNE possibly could aid in its localization to the plasma membrane, increasing interactions with the insulin receptor and inhibiting insulin action. Calumenin, a protein involved in the regulation of calcium flux out of the ER, is also an intriguing target of carbonylation as it has been shown that ER stress is activated in obesity (23, 69). During conditions of ER stress, misfolded proteins accumulate in the ER lumen and initiate the unfolded protein response and the activation of JNK, which is known to increase serine phosphorylation of insulin receptor substrate-1 (23). As ER stress can be initiated by calcium release from the ER, the potential inactivation of calumenin by 4-HNE could contribute to the unfolded protein response and JNK activation in an indirect manor (70). In addition, the modification of eukaryotic elongation factor 1α-1 (eEF1α1) could contribute to insulin resistance through the activation of a similar stress response. This protein has been shown to be involved in activating apoptosis under lipotoxic conditions in non-adipose cells (71). Although adipocytes do not undergo apoptosis in response to high amounts of lipid, it is possible that eEF1α1 is involved in activating other stress responses in adipocytes in obesity. Although these proteins are intriguing candidates for being targets of modification by 4-HNE or other lipid peroxidation products, additional studies are necessary to determine the specific modifications and potential effects in each case.

The decreased amount of GSTA4 protein (~3–4-fold) in adipose tissue of obese mice seen in this study (Fig. 4) is consistent with published microarray data demonstrating decreased GSTA4 mRNA expression in adipose tissue of obese C57Bl/6J mice (72). GSTA4 has been shown previously to be the primary GST isozyme responsible for metabolizing 4-HNE (47, 48). As such, a 3–4-fold decrease in GSTA4 in adipose cells would presumably contribute to increased accumulation of 4-HNE and other lipid peroxidation products, resulting in elevated protein carbonylation as observed in this study. Further investigation is needed to determine whether protein carbonylation and GSTA4 abundance are components linking obesity to insulin resistance.

Acknowledgments—We thank all members of the Bernlohr and Griffin research groups who provided helpful suggestions regarding this work and specifically Lisa Smith and Wendy Wright for maintenance and care of the animals and Mikel Roe for assistance with instrument methods. We also thank Dr. LeeAnn Higgins and the staff of the University of Minnesota Center for Mass Spectrometry and Proteomics for instruction on instrument operation and the Minnesota Supercomputing Institute for maintenance of the SEQUEST cluster.

* This work was supported by National Institutes of Health Grant DK053189, the Minnesota Agricultural Experiment Station, and the Minnesota Obesity Center (to D. A. B.); by NHLBI, National Institutes of Health Grant T32 HL07741 (to P. A. G.); by National Institutes of Health Grant AG025371 (to T. J. G.); and by National Center for Research Resources Grant P20 RR17699-01 from the Center of Biomedical Research Excellence (to M. J. P.). The costs of publication of this article were defrayed in part by the payment of page charges. This article must therefore be hereby marked "*advertisement*" in accordance with 18 U.S.C. Section 1734 solely to indicate this fact.

S The on-line version of this article (available at http://www.mcponline.org) contains supplemental material.

¶ To whom correspondence should be addressed: Dept. of Biochemistry, Molecular Biology and Biophysics, University of Minnesota-Twin Cities, 321 Church St. S. E., Minneapolis, MN 55455. Tel.: 612-624-2712; Fax: 612-625-2163; E-mail: bernl001@umn.edu.

REFERENCES

1. Finkel, T., and Holbrook, N. J. (2000) Oxidants, oxidative stress and the biology of ageing. *Nature* **408,** 239–247
2. Smith, M. A., Rottkamp, C. A., Nunomura, A., Raina, A. K., and Perry, G. (2000) Oxidative stress in Alzheimer's disease. *Biochim. Biophys. Acta* **1502,** 139–144

3. Winkler, B. S., Boulton, M. E., Gottsch, J. D., and Sternberg, P. (1999) Oxidative damage and age-related macular degeneration. *Mol. Vis.* **5,** 32
4. Barreiro, E., de la Puente, B., Minguella, J., Corominas, J. M., Serrano, S., Hussain, S. N., and Gea, J. (2005) Oxidative stress and respiratory muscle dysfunction in severe chronic obstructive pulmonary disease. *Am. J. Respir. Crit. Care Med.* **171,** 1116–1124
5. Furukawa, S., Fujita, T., Shimabukuro, M., Iwaki, M., Yamada, Y., Nakajima, Y., Nakayama, O., Makishima, M., Matsuda, M., and Shimomura, I. (2004) Increased oxidative stress in obesity and its impact on metabolic syndrome. *J. Clin. Investig.* **114,** 1752–1761
6. Uchida, K. (2003) 4-Hydroxy-2-nonenal: a product and mediator of oxidative stress. *Prog. Lipid Res.* **42,** 318–343
7. Benedetti, A., Comporti, M., and Esterbauer, H. (1980) Identification of 4-hydroxynonenal as a cytotoxic product originating from the peroxidation of liver microsomal lipids. *Biochim. Biophys. Acta* **620,** 281–296
8. Lee, S. H., and Blair, I. A. (2000) Characterization of 4-oxo-2-nonenal as a novel product of lipid peroxidation. *Chem. Res. Toxicol.* **13,** 698–702
9. Sayre, L. M., Lin, D., Yuan, Q., Zhu, X., and Tang, X. (2006) Protein adducts generated from products of lipid oxidation: focus on HNE and ONE. *Drug Metab. Rev.* **38,** 651–675
10. Honzatko, A., Brichac, J., Murphy, T. C., Reberg, A., Kubatova, A., Smoliakova, I. P., and Picklo, M. J., Sr. (2005) Enantioselective metabolism of trans-4-hydroxy-2-nonenal by brain mitochondria. *Free Radic. Biol. Med.* **39,** 913–924
11. Canuto, R. A., Ferro, M., Muzio, G., Bassi, A. M., Leonarduzzi, G., Maggiora, M., Adamo, D., Poli, G., and Lindahl, R. (1994) Role of aldehyde metabolizing enzymes in mediating effects of aldehyde products of lipid peroxidation in liver cells. *Carcinogenesis* **15,** 1359–1364
12. Sharma, R., Yang, Y., Sharma, A., Awasthi, S., and Awasthi, Y. C. (2004) Antioxidant role of glutathione S-transferases: protection against oxidant toxicity and regulation of stress-mediated apoptosis. *Antioxid. Redox Signal.* **6,** 289–300
13. Carini, M., Aldini, G., and Facino, R. M. (2004) Mass spectrometry for detection of 4-hydroxy-trans-2-nonenal (HNE) adducts with peptides and proteins. *Mass Spectrom. Rev.* **23,** 281–305
14. Oberley, T. D., Toyokuni, S., and Szweda, L. I. (1999) Localization of hydroxynonenal protein adducts in normal human kidney and selected human kidney cancers. *Free Radic. Biol. Med.* **27,** 695–703
15. Miyake, H., Kadoya, A., and Ohyashiki, T. (2003) Increase in molecular rigidity of the protein conformation of brain Na^+-K^+-ATPase by modification with 4-hydroxy-2-nonenal. *Biol. Pharm. Bull.* **26,** 1652–1656
16. Yang, J. H., Yang, E. S., and Park, J. W. (2004) Inactivation of $NADP^+$-dependent isocitrate dehydrogenase by lipid peroxidation products. *Free Radic. Res.* **38,** 241–249
17. Liu, W., Akhand, A. A., Kato, M., Yokoyama, I., Miyata, T., Kurokawa, K., Uchida, K., and Nakashima, I. (1999) 4-Hydroxynonenal triggers an epidermal growth factor receptor-linked signal pathway for growth inhibition. *J. Cell Sci.* **112,** 2409–2417
18. Levonen, A. L., Landar, A., Ramachandran, A., Ceaser, E. K., Dickinson, D. A., Zanoni, G., Morrow, J. D., and Darley-Usmar, V. M. (2004) Cellular mechanisms of redox cell signalling: role of cysteine modification in controlling antioxidant defences in response to electrophilic lipid oxidation products. *Biochem. J.* **378,** 373–382
19. Zhang, H., Liu, H., Dickinson, D. A., Liu, R. M., Postlethwait, E. M., Laperche, Y., and Forman, H. J. (2006) γ-Glutamyl transpeptidase is induced by 4-hydroxynonenal via EpRE/Nrf2 signaling in rat epithelial type II cells. *Free Radic. Biol. Med.* **40,** 1281–1292
20. West, J. D., and Marnett, L. J. (2005) Alterations in gene expression induced by the lipid peroxidation product, 4-hydroxy-2-nonenal. *Chem. Res. Toxicol.* **18,** 1642–1653
21. Carbone, D. L., Doorn, J. A., and Petersen, D. R. (2004) 4-Hydroxynonenal regulates 26S proteasomal degradation of alcohol dehydrogenase. *Free Radic. Biol. Med.* **37,** 1430–1439
22. Marques, C., Pereira, P., Taylor, A., Liang, J. N., Reddy, V. N., Szweda, L. I., and Shang, F. (2004) Ubiquitin-dependent lysosomal degradation of the HNE-modified proteins in lens epithelial cells. *FASEB J.* **18,** 1424–1426
23. Ozcan, U., Cao, Q., Yilmaz, E., Lee, A. H., Iwakoshi, N. N., Ozdelen, E., Tuncman, G., Gorgun, C., Glimcher, L. H., and Hotamisligil, G. S. (2004) Endoplasmic reticulum stress links obesity, insulin action, and type 2 diabetes. *Science* **306,** 457–461
24. Houstis, N., Rosen, E. D., and Lander, E. S. (2006) Reactive oxygen species have a causal role in multiple forms of insulin resistance. *Nature* **440,** 944–948
25. Talior, I., Yarkoni, M., Bashan, N., and Eldar-Finkelman, H. (2003) Increased glucose uptake promotes oxidative stress and PKC-δ activation in adipocytes of obese, insulin-resistant mice. *Am. J. Physiol.* **285,** E295–E302
26. Lin, Y., Berg, A. H., Iyengar, P., Lam, T. K., Giacca, A., Combs, T. P., Rajala, M. W., Du, X., Rollman, B., Li, W., Hawkins, M., Barzilai, N., Rhodes, C. J., Fantus, I. G., Brownlee, M., and Scherer, P. E. (2005) The hyperglycemia-induced inflammatory response in adipocytes: the role of reactive oxygen species. *J. Biol. Chem.* **280,** 4617–4626
27. Soares, A. F., Guichardant, M., Cozzone, D., Bernoud-Hubac, N., Bouzaidi-Tiali, N., Lagarde, M., and Geloen, A. (2005) Effects of oxidative stress on adiponectin secretion and lactate production in 3T3-L1 adipocytes. *Free Radic. Biol. Med.* **38,** 882–889
28. Bays, H., Mandarino, L., and DeFronzo, R. A. (2004) Role of the adipocyte, free fatty acids, and ectopic fat in pathogenesis of type 2 diabetes mellitus: peroxisomal proliferator-activated receptor agonists provide a rational therapeutic approach. *J. Clin. Endocrinol. Metab.* **89,** 463–478
29. Mirzaei, H., and Regnier, F. (2005) Affinity chromatographic selection of carbonylated proteins followed by identification of oxidation sites using tandem mass spectrometry. *Anal. Chem.* **77,** 2386–2392
30. Surwit, R. S., Kuhn, C. M., Cochrane, C., McCubbin, J. A., and Feinglos, M. N. (1988) Diet-induced type II diabetes in C57BL/6J mice. *Diabetes* **37,** 1163–1167
31. Hertzel, A. V., Smith, L. A., Berg, A. H., Cline, G. W., Shulman, G. I., Scherer, P. E., and Bernlohr, D. A. (2006) Lipid metabolism and adipokine levels in fatty acid binding protein null and transgenic mice. *Am. J. Physiol.* **290,** E814–E823
32. Wessel, D., and Flugge, U. I. (1984) A method for the quantitative recovery of protein in dilute solution in the presence of detergents and lipids. *Anal. Biochem.* **138,** 141–143
33. Xie, H., Bandhakavi, S., and Griffin, T. J. (2005) Evaluating preparative isoelectric focusing of complex peptide mixtures for tandem mass spectrometry-based proteomics: a case study in profiling chromatin-enriched subcellular fractions in Saccharomyces cerevisiae. *Anal. Chem.* **77,** 3198–3207
34. Xie, H., Rhodus, N. L., Griffin, R. J., Carlis, J. V., and Griffin, T. J. (2005) A catalogue of human saliva proteins identified by free flow electrophoresis-based peptide separation and tandem mass spectrometry. *Mol. Cell. Proteomics* **4,** 1826–1830
35. Eng, J. K., McCormack, A. L., and Yates, J. R. (1994) An approach to correlate tandem mass spectral data of peptides with amino acid sequences in a protein database. *J. Am. Soc. Mass Spectrom.* **5,** 976–989
36. Peng, J., Elias, J. E., Thoreen, C. C., Licklider, L. J., and Gygi, S. P. (2003) Evaluation of multidimensional chromatography coupled with tandem mass spectrometry (LC/LC-MS/MS) for large-scale protein analysis: the yeast proteome. *J. Proteome Res.* **2,** 43–50
37. Keller, A., Nesvizhskii, A. I., Kolker, E., and Aebersold, R. (2002) Empirical statistical model to estimate the accuracy of peptide identifications made by MS/MS and database search. *Anal. Chem.* **74,** 5383–5392
38. Xie, H., and Griffin, T. J. (2006) Trade-off between high sensitivity and increased potential for false positive peptide sequence matches using a two-dimensional linear ion trap for tandem mass spectrometry-based proteomics. *J. Proteome Res.* **5,** 1003–1009
39. Kane, C. D., Coe, N. R., Vanlandingham, B., Krieg, P., and Bernlohr, D. A. (1996) Expression, purification, and ligand-binding analysis of recombinant keratinocyte lipid-binding protein (MAL-1), an intracellular lipid-binding found overexpressed in neoplastic skin cells. *Biochemistry* **35,** 2894–2900
40. Xu, Z. H., Buelt, M. K., Banaszak, L. J., and Bernlohr, D. A. (1991) Expression, purification, and crystallization of the adipocyte lipid binding protein. *J. Biol. Chem.* **266,** 14367–14370
41. Jenkins-Kruchten, A. E., Bennaars-Eiden, A., Ross, J. R., Shen, W. J., Kraemer, F. B., and Bernlohr, D. A. (2003) Fatty acid-binding protein-hormone-sensitive lipase interaction. Fatty acid dependence on binding. *J. Biol. Chem.* **278,** 47636–47643
42. Matarese, V., Buelt, M. K., Chinander, L. L., and Bernlohr, D. A. (1990) Purification of adipocyte lipid-binding protein from human and murine cells. *Methods Enzymol.* **189,** 363–369
43. Bennaars-Eiden, A., Higgins, L., Hertzel, A. V., Kapphahn, R. J., Ferrington, D. A., and Bernlohr, D. A. (2002) Covalent modification of epithelial fatty

acid-binding protein by 4-hydroxynonenal in vitro and in vivo. Evidence for a role in antioxidant biology. *J. Biol. Chem.* **277,** 50693–50702
44. Kane, C. D., and Bernlohr, D. A. (1996) A simple assay for intracellular lipid-binding proteins using displacement of 1-anilinonaphthalene 8-sulfonic acid. *Anal. Biochem.* **233,** 197–204
45. Yan, L. J., Orr, W. C., and Sohal, R. S. (1998) Identification of oxidized proteins based on sodium dodecyl sulfate-polyacrylamide gel electrophoresis, immunochemical detection, isoelectric focusing, and microsequencing. *Anal. Biochem.* **263,** 67–71
46. Stadtman, E. R. (1992) Protein oxidation and aging. *Science* **257,** 1220–1224
47. Yang, Y., Trent, M. B., He, N., Lick, S. D., Zimniak, P., Awasthi, Y. C., and Boor, P. J. (2004) Glutathione-S-transferase A4–4 modulates oxidative stress in endothelium: possible role in human atherosclerosis. *Atherosclerosis* **173,** 211–221
48. Engle, M. R., Singh, S. P., Czernik, P. J., Gaddy, D., Montague, D. C., Ceci, J. D., Yang, Y., Awasthi, S., Awasthi, Y. C., and Zimniak, P. (2004) Physiological role of mGSTA4–4, a glutathione S-transferase metabolizing 4-hydroxynonenal: generation and analysis of mGsta4 null mouse. *Toxicol. Appl. Pharmacol.* **194,** 296–308
49. Carbone, D. L., Doorn, J. A., Kiebler, Z., Sampey, B. P., and Petersen, D. R. (2004) Inhibition of Hsp72-mediated protein refolding by 4-hydroxy-2-nonenal. *Chem. Res. Toxicol.* **17,** 1459–1467
50. Carbone, D. L., Doorn, J. A., Kiebler, Z., Ickes, B. R., and Petersen, D. R. (2005) Modification of heat shock protein 90 by 4-hydroxynonenal in a rat model of chronic alcoholic liver disease. *J. Pharmacol. Exp. Ther.* **315,** 8–15
51. Pappin, D. J., Hojrup, P., and Bleasby, A. J. (1993) Rapid identification of proteins by peptide-mass fingerprinting. *Curr. Biol.* **3,** 327–332
52. Gelfi, C., De Palma, S., Ripamonti, M., Eberini, I., Wait, R., Bajracharya, A., Marconi, C., Schneider, A., Hoppeler, H., and Cerretelli, P. (2004) New aspects of altitude adaptation in Tibetans: a proteomic approach. *FASEB J.* **18,** 612–614
53. Castegna, A., Aksenov, M., Thongboonkerd, V., Klein, J. B., Pierce, W. M., Booze, R., Markesbery, W. R., and Butterfield, D. A. (2002) Proteomic identification of oxidatively modified proteins in Alzheimer's disease brain. Part II: dihydropyrimidinase-related protein 2, β-enolase and heat shock cognate 71. *J. Neurochem.* **82,** 1524–1532
54. Hohoff, C., Borchers, T., Rustow, B., Spener, F., and van Tilbeurgh, H. (1999) Expression, purification, and crystal structure determination of recombinant human epidermal-type fatty acid binding protein. *Biochemistry* **38,** 12229–12239
55. Gutierrez-Gonzalez, L. H., Ludwig, C., Hohoff, C., Rademacher, M., Hanhoff, T., Ruterjans, H., Spener, F., and Lucke, C. (2002) Solution structure and backbone dynamics of human epidermal-type fatty acid-binding protein (E-FABP). *Biochem. J.* **364,** 725–737
56. Reese-Wagoner, A., Thompson, J., and Banaszak, L. (1999) Structural properties of the adipocyte lipid binding protein. *Biochim. Biophys. Acta* **1441,** 106–116
57. LaLonde, J. M., Bernlohr, D. A., and Banaszak, L. J. (1994) X-ray crystallographic structures of adipocyte lipid-binding protein complexed with palmitate and hexadecanesulfonic acid. Properties of cavity binding sites. *Biochemistry* **33,** 4885–4895
58. Xu, Z., Bernlohr, D. A., and Banaszak, L. J. (1993) The adipocyte lipid-binding protein at 1.6-Å resolution. Crystal structures of the apoprotein and with bound saturated and unsaturated fatty acids. *J. Biol. Chem.* **268,** 7874–7884
59. LaLonde, J. M., Levenson, M. A., Roe, J. J., Bernlohr, D. A., and Banaszak, L. J. (1994) Adipocyte lipid-binding protein complexed with arachidonic acid. Titration calorimetry and X-ray crystallographic studies. *J. Biol. Chem.* **269,** 25339–25347
60. Buelt, M. K., and Bernlohr, D. A. (1990) Modification of the adipocyte lipid binding protein by sulfhydryl reagents and analysis of the fatty acid binding domain. *Biochemistry* **29,** 7408–7413
61. Doorn, J. A., and Petersen, D. R. (2002) Covalent modification of amino acid nucleophiles by the lipid peroxidation products 4-hydroxy-2-nonenal and 4-oxo-2-nonenal. *Chem. Res. Toxicol.* **15,** 1445–1450
62. Hiratsuka, A., Tobita, K., Saito, H., Sakamoto, Y., Nakano, H., Ogura, K., Nishiyama, T., and Watabe, T. (2001) (S)-Preferential detoxification of 4-hydroxy-2(E)-nonenal enantiomers by hepatic glutathione S-transferase isoforms in guinea-pigs and rats. *Biochem. J.* **355,** 237–244
63. Wood, Z. A., Schroder, E., Robin Harris, J., and Poole, L. B. (2003) Structure, mechanism and regulation of peroxiredoxins. *Trends. Biochem. Sci.* **28,** 32–40
64. Drevet, J. R. (2006) The antioxidant glutathione peroxidase family and spermatozoa: a complex story. *Mol. Cell. Endocrinol.* **250,** 70–79
65. Kang, S. W., Chae, H. Z., Seo, M. S., Kim, K., Baines, I. C., and Rhee, S. G. (1998) Mammalian peroxiredoxin isoforms can reduce hydrogen peroxide generated in response to growth factors and tumor necrosis factor-α. *J. Biol. Chem.* **273,** 6297–6302
66. Jin, D. Y., Chae, H. Z., Rhee, S. G., and Jeang, K. T. (1997) Regulatory role for a novel human thioredoxin peroxidase in NF-κB activation. *J. Biol. Chem.* **272,** 30952–30961
67. Kretz-Remy, C., Mehlen, P., Mirault, M. E., and Arrigo, A. P. (1996) Inhibition of IκB-α phosphorylation and degradation and subsequent NF-κB activation by glutathione peroxidase overexpression. *J. Cell Biol.* **133,** 1083–1093
68. He, H. J., Kole, S., Kwon, Y. K., Crow, M. T., and Bernier, M. (2003) Interaction of filamin A with the insulin receptor alters insulin-dependent activation of the mitogen-activated protein kinase pathway. *J. Biol. Chem.* **278,** 27096–27104
69. Jung, D. H., Mo, S. H., and Kim, D. H. (2006) Calumenin, a multiple EF-hands Ca^{2+}-binding protein, interacts with ryanodine receptor-1 in rabbit skeletal sarcoplasmic reticulum. *Biochem. Biophys. Res. Commun.* **343,** 34–42
70. DuRose, J. B., Tam, A. B., and Niwa, M. (2006) Intrinsic capacities of molecular sensors of the unfolded protein response to sense alternate forms of endoplasmic reticulum stress. *Mol. Biol. Cell* **17,** 3095–3107
71. Borradaile, N. M., Buhman, K. K., Listenberger, L. L., Magee, C. J., Morimoto, E. T., Ory, D. S., and Schaffer, J. E. (2006) A critical role for eukaryotic elongation factor 1A-1 in lipotoxic cell death. *Mol. Biol. Cell* **17,** 770–778
72. Moraes, R. C., Blondet, A., Birkenkamp-Demtroeder, K., Tirard, J., Orntoft, T. F., Gertler, A., Durand, P., Naville, D., and Begeot, M. (2003) Study of the alteration of gene expression in adipose tissue of diet-induced obese mice by microarray and reverse transcription-polymerase chain reaction analyses. *Endocrinology* **144,** 4773–4782